Pergamon

Geochimica et Cosmochimica Acta, Vol. 68, No. 16, pp. 3423–3438, 2004

0016-7037/04 $30.00 + .00

doi:10.1016/j.gca.2004.01.013

Oxygen isotope heterogeneity in chondrules from the Mokoia CV3 carbonaceous chondrite

RHIAN H. JONES,[1,*] LAURIE A. LESHIN,[2] YUNBIN GUAN,[2] ZACHARY D. SHARP,[3] TOMASZ DURAKIEWICZ,[3,4] and ALAN J. SCHILK[5]

[1]Institute of Meteoritics, Department of Earth and Planetary Sciences, University of New Mexico, Albuquerque, NM 87131, USA
[2]Department of Geological Sciences and Center for Meteorite Studies, Arizona State University, Tempe, AZ 85287-1404, USA
[3]Department of Earth and Planetary Sciences, University of New Mexico, Albuquerque, NM 87131, USA
[4]Institute of Physics, University of Maria Curie, Sklodowska, 20-031 Lublin, Poland
[5]Idaho National Engineering and Environmental Laboratory, P.O. Box 1625, Idaho Falls, ID 83415-7139, USA

(*Received July* 8, 2003; *accepted in revised form January* 8, 2004)

Abstract—We report a study of the oxygen isotope ratios of chondrules and their constituent mineral grains from the Mokoia, oxidized CV3 chondrite. Bulk oxygen isotope ratios of 23 individual chondrules were determined by laser ablation fluorination, and oxygen isotope ratios of individual grains, mostly olivine, were obtained in situ on polished mounts using secondary ion mass spectrometry (SIMS). Our results can be compared with data obtained previously for the oxidized CV3 chondrite, Allende. Bulk oxygen isotope ratios of Mokoia chondrules form an array on an oxygen three-isotope plot that is subparallel to, and slightly displaced from, the CCAM (carbonaceous chondrite anhydrous minerals) line. The best-fit line for all CV3 chondrite chondrules has a slope of 0.99, and is displaced significantly (by $\delta^{17}O \sim -2.5‰$) from the Young and Russell slope-one line for unaltered calcium-aluminum-rich inclusion (CAI) minerals. Oxygen isotope ratios of many bulk CAIs also lie on the CV-chondrule line, which is the most relevant oxygen isotope array for most CV chondrite components. Bulk oxygen isotope ratios of most chondrules in Mokoia have $\delta^{18}O$ values around 0‰, and olivine grains in these chondrules have similar oxygen isotope ratios to their bulk values. In general, it appears that chondrule mesostases have higher $\delta^{18}O$ values than olivines in the same chondrules. Our bulk chondrule data spread to lower $\delta^{18}O$ values than any ferromagnesian chondrules that have been measured previously. Two chondrules with the lowest bulk $\delta^{18}O$ values ($-7.5‰$ and $-11.7‰$) contain olivine grains that display an extremely wide range of oxygen isotope ratios, down to $\delta^{17}O$, $\delta^{18}O$ around -50‰ in one chondrule. In these chondrules, there are no apparent relict grains, and essentially no relationships between olivine compositions, which are homogeneous, and oxygen isotopic compositions of individual grains. Heterogeneity of oxygen isotope ratios within these chondrules may be the result of incorporation of relict grains from objects such as amoeboid olivine aggregates, followed by solid-state chemical diffusion without concomitant oxygen equilibration. Alternatively, oxygen isotope exchange between an ^{16}O-rich precursor and an ^{16}O-poor gas may have taken place during chondrule formation, and these chondrules may represent partially equilibrated systems in which isotopic heterogeneities became frozen into the crystallizing olivine grains. If this is the case, we can infer that the earliest nebular solids from which chondrules formed had $\delta^{17}O$ and $\delta^{18}O$ values around -50‰, similar to those observed in refractory inclusions.

1. INTRODUCTION

Chondritic meteorites provide us with direct information about the early history of the solar system. To understand the processes that took place at this time, it is necessary to understand the combined chemical, petrologic, and isotopic information carried by primitive components of chondrites such as chondrules and calcium-, aluminum-rich inclusions (CAIs). The role of oxygen isotope studies is important to this overall picture because chondritic components record considerable oxygen isotopic complexity that must be unraveled to place chondrule and CAI formation in their appropriate contexts.

Refractory components, including CAIs and amoeboid olivine aggregates (AOAs) from all major chondrite groups (carbonaceous, ordinary, enstatite) have ~5% enrichments in ^{16}O compared with most other components of chondrites (Clayton et al., 1977; McKeegan et al., 1998; Hiyagon and Hashimoto, 1999; Guan et al., 2000; Fagan et al., 2001). This suggests that CAIs from different samples shared common origins. Because refractory components are rare, constituting less than 1 volume % of most chondrite groups, this has led to speculation that these objects sample a restricted environment in the solar nebula, that differs from the more volumetrically important chondrule-forming region (McKeegan et al., 1998; Krot et al., 2002). However, the number of detailed studies of oxygen isotope variations in chondrules is limited. A detailed knowledge of oxygen isotopic relationships within the chondrule population is critical to interpreting not only the relationships between chondrules and refractory inclusions, but also the evolution of nebular solids in general.

Previous studies have shown that within the CV3 chondrite group, the oxygen isotope ratios of bulk chondrules and CAIs lie along an array that has a slope close to one on an oxygen three-isotope plot (e.g., Clayton, 1993). Oxygen isotope ratios of individual forsterite grains in CV chondrites also lie close to this CCAM (carbonaceous chondrite anhydrous minerals) line (Weinbruch et al., 1993; Choi et al., 2000). In this paper we report a detailed study of the oxygen isotope ratios of a suite of 23 chondrules extracted from the oxidized CV3 chondrite, Mokoia, including both bulk chondrule measurements and in situ analyses of their constituent grains. The chondrules are part

* Author to whom correspondence should be addressed (rjones@unm.edu).

of a suite of 94 chondrules from Mokoia that were separated for measurements of bulk chemistry by instrumental neutron activation analysis (Schilk, 1991), the chemistry and petrology of which will be discussed in detail elsewhere. The chondrule suite described in this study covers a wide range of compositional and textural types, including FeO-poor, FeO-rich, and Al-rich chondrules, and porphyritic olivine (PO), porphyritic olivine/pyroxene (POP), porphyritic pyroxene (PP), and barred olivine (BO) textural types as well as one compound chondrule. Measuring oxygen isotope ratios in both bulk chondrules and on high-spatial resolution, in situ spots on the same chondrules, places constraints on the heterogeneity of oxygen isotopes in the chondrule-forming region of the solar nebula. Our observations include a wider range of bulk chondrule oxygen isotope ratios than has been observed previously in any other chondrite, and measurements of oxygen isotopic heterogeneity within individual chondrules that is unprecedented for chondrules.

Most studies of chondrules and CAIs in CV chondrites have focused on the oxidized CV3 chondrite, Allende. Mokoia is a similar chondrite to Allende in many respects, for example, both have a lower matrix/chondrule ratio (~0.7) than other members of the oxidized CV chondrites (~1.2: McSween, 1977a). However, there are also some important differences between them. (1) Mokoia is a relatively unaltered chondrite that shows minimal effects of thermal metamorphism (McSween, 1977a): matrix olivines in Mokoia have a more variable fayalite content than those in Allende (Peck, 1983; Scott et al., 1988). Mokoia was classified as a breccia of petrologic types 3.0-3.2 by Guimon et al. (1995), whereas Allende was classified as 3.2-3.3. (2) Mokoia contains ubiquitous phyllosilicates in matrix, CAIs, and chondrule mesostases, showing that it underwent an episode of aqueous alteration (Cohen et al., 1983; Tomeoka and Buseck, 1990; Kimura and Ikeda, 1998). In contrast, phyllosilicates have not been observed in Allende, although rare occurrences of various other, hydrous phases have been reported (Tomeoka and Buseck, 1982; Kimura and Ikeda, 1996; Brearley, 1997). (3) Chondrules in Allende contain olivine grains that have wide, FeO-rich rims that have been interpreted as the result of either nebular alteration (Peck and Wood, 1987; Hua et al., 1988; Weinbruch et al., 1990) or parent body processing (Krot et al., 1997). Similar rims have not been reported in Mokoia chondrules. In summary, by studying chondrules in Mokoia, we are thus able to compare the properties of two oxidized CV chondrites that have experienced different alteration environments. Although it appears that both Allende and Mokoia have experienced episodes of aqueous alteration and thermal metamorphism (Krot et al., 1995, 1997; Hutcheon et al., 1998), the secondary history of Allende, in which phyllosilicate minerals were dehydrated, appears to be more complex than that of Mokoia. Many of the chondrules in Mokoia show little evidence of metamorphic equilibration. Hence we are more likely to observe the properties of primary chondrule-forming processes in Mokoia and gain more direct insights into the distribution of oxygen isotopes in chondrule-forming regions of the solar nebula.

2. ANALYTICAL TECHNIQUES

Twenty-three chondrules that had been disaggregated from Mokoia (Schilk, 1991) were selected for oxygen isotope analysis (Table 1). Fifteen of these were selected because they were large (masses 5 to 21 mg, mean diameters 1.5 to 2.3 mm). For these, we cut the chondrule into two pieces using a wafering blade and made polished mounts set in epoxide from one part. The polished faces were used to determine petrology as well as for in situ oxygen isotope measurements. Secondary electron and back-scattered electron imaging, plus cathodoluminescence mapping, were performed on the JEOL 5800LV scanning electron microscope (SEM) at the University of New Mexico. Quantitative analyses of mineral phases were performed using the JEOL 733 Superprobe electron microprobe, also at the University of New Mexico, with operating conditions of 15 kV and a beam current of 20 nA.

Bulk O isotope ratios of 23 chondrules were measured, including the 15 chondrules for which the petrology was determined and eight additional smaller chondrules (masses 2.1-4.8 mg). Bulk oxygen isotope ratios of the chondrules were determined by a laser ablation technique using a Finnigan MAT Delta Plus XL mass spectrometer at the University of New Mexico. Chondrule fragments, or whole chondrules, ~2 mg in mass, were analyzed as O_2 using the laser extraction technique described by Sharp (1990, 1995). Duplicate analyses were obtained for two of the larger chondrules (34 and 13C). A 13x molecular sieve was used to remove excess NF_3. All terrestrial analyses measured have $\Delta^{17}O$ values of $0 \pm 0.1‰$. Analytical errors on individual measurements are $\pm$ 0.2‰ for $\delta^{17}O$ and $\pm$ 0.1‰ for $\delta^{18}O$.

In situ oxygen isotope analyses were made for five of the chondrules using the Cameca IMS 6f ion microprobe (secondary ion mass spectrometry [SIMS]) at Arizona State University, on polished mounts comprising a single chondrule and a San Carlos olivine standard. A 0.2-0.34-nA beam of Cs^+ was focused into a spot ~20 μm in diameter in aperture illumination mode. Secondary ions were collected by peak-jumping into either a Faraday cup ($^{16}O^-$) or electron multiplier ($^{17}O^-$ and $^{18}O^-$) at a mass resolving power of ~6500, easily resolving the $^{16}OH^-$ interference on $^{17}O^-$. Uncertainties on individual analyses, including analytical errors and statistical variation on repeated analyses of the standard, are ~1.5-5‰ (2σ). The magnitudes of matrix effects are small (less than a few ‰) under our analysis conditions. No corrections for such effects have been made.

3. RESULTS

The chondrules studied include a variety of textural and compositional types, summarized in Table 1. Mean Fa contents of olivine grains, determined from random analyses of olivine within individual chondrules, range from 0.5 to 12 mol%. Mean Fs contents of low-Ca pyroxenes range from 0.8 to 2.4 mol%. Most of the chondrules show little or no evidence of metamorphism, in the form of Fe-Mg diffusion along grain boundaries and cracks in olivine grains at the outer edges of chondrules. Some of the chondrules show evidence of more extensive metamorphism (noted in Table 1), with significant Fe-Mg diffusion: these include chondrules 24A and, especially, 33 and 5C, in which mean Fa contents are higher than corresponding Fs contents of low-Ca pyroxene.

Most of the chondrules studied are FeO-poor, olivine-rich, porphyritic chondrules. They contain rounded aggregates that consist predominantly of magnetite, and that we interpret to be the products of oxidation of Fe,Ni metal that was originally present when the chondrules formed (Housley and Cirlin, 1983; Krot et al., 1995; Choi et al., 2000). Figure 1 shows examples of chondrule textures, as represented by the five chondrules selected for SIMS analyses. Chondrules 11 (Fig. 1a,b) and 12 (Fig. 1c,d) are fine-grained, FeO-poor, porphyritic chondrules with mean grain sizes around 30 μm. Both have rounded outlines in cross-section but are irregular in shape overall. Chondrule 11 contains predominantly olivine phenocrysts, whereas chondrule 12 is predominantly olivine-rich, but has an outer mantle in which coarser laths of low-Ca pyroxene occur, elongated perpendicular to the outer edge of the chondrule. The

Table 1. Chondrule properties and bulk chondrule oxygen isotope ratios.

Chondrule	Textural type[a]	Mass (mg)	Mean Fa (mol%)	Mean Fs[b] (mol%)	$\delta^{18}O$ (‰)	2σ	$\delta^{17}O$ (‰)	2σ	$\Delta^{17}O$ (‰)	Degree metam.[c]
11	fine-grained PO	10.07	1.49	—	−7.48	0.1	−10.63	0.2	−6.74	minor
12	fine-grained POP	8.02	1.08	0.86	−11.74	0.1	−14.56	0.2	−8.46	minor
13	PO	6.77	1.18		1.70	0.1	−2.19	0.2	−3.08	minor
15	plag-rich POP	5.17	0.97	1.24	2.70	0.1	−1.32	0.2	−2.73	none
20	not known	2.08	—	—	1.93	0.1	−1.35	0.2	−2.35	
33	PO/POP	6.76	6.44	1.81	−0.63	0.1	−4.42	0.2	−4.09	significant
34	POP	16.35	4.11	0.80	−0.35	0.1	−3.75	0.2	−3.57	minor
					−0.91	0.1	−4.51	0.2	−4.04	
36	FeO-rich BO	5.17	12.0	—	6.00	0.1	2.69	0.2	−0.43	none
74	not known	2.17	—	—	−1.46	0.1	−4.63	0.2	−3.87	
80	not known	2.05	—	—	5.31	0.1	0.18	0.2	−2.58	
22A	not known	4.75	—	—	0.44	0.1	−3.86	0.2	−4.09	
23A	plag-rich POP	6.82	1.04	1.10	4.37	0.1	−0.72	0.2	−2.99	minor
24A	PO	14.31	3.62	0.98	0.71	0.1	−2.58	0.2	−2.95	moderate
26A	not known	3.81	—	—	−4.41	0.1	−8.20	0.2	−5.91	
1C	not known	2.82	—	—	−1.27	0.1	−4.99	0.2	−4.33	
3C	not known	3.96	—	—	−1.82	0.1	−5.32	0.2	−4.37	
5C	micro PO/POP	7.03	2.72	1.21	−2.37	0.1	−5.63	0.2	−4.39	significant
7C	PO	5.77	1.61	—	−2.86	0.1	−6.06	0.2	−4.58	none
9C	not known	3.85	—	—	−0.73	0.1	−4.71	0.2	−4.33	
10C	POP	10.84	1.03	1.15	−0.80	0.1	−4.01	0.2	−3.59	none
12C	PP	14.85	3.15	2.35	2.39	0.1	−1.51	0.2	−2.75	none
13C[d]	compound BO/PO	21.07	0.76 (BO)	0.80 (BO)	−0.66	0.1	−4.37	0.2	−4.03	minor
			0.81 (PO)	1.33 (PO)	−1.71	0.1	−4.55	0.2	−3.66	
14C	Al-rich PO	15.01	0.52	—	0.96	0.1	−3.08	0.2	−3.58	none

[a] PO = porphyritic olivine; POP = porphyritic olivine and pyroxene; PP = porphyritic pyroxene; BO = barred olivine.
[b] Low-Ca pyroxene only.
[c] Degree of metamorphism as indicated by FeO zoning along cracks and grain boundaries in olivine and low-Ca pyroxene.
[d] The two oxygen isotope analyses for 13C are both bulk samples that may include both the BO and the PO chondrule.

outer region is also richer in mesostasis than the inner, olivine-rich zone. For both chondrules 11 and 12, the mesostasis consists predominantly of a crystalline intergrowth of diopside and anorthite. Minor enrichments in FeO at the edges of olivine grains in chondrule 11 may be the result of either igneous zoning or mild metamorphism. Chondrule 12 has clearly undergone a minor degree of secondary metamorphism that is observable in the outer region, as well as in a porous zone in the center, where olivine is slightly enriched in FeO (Fig. 1d).

Chondrule 34 is a coarser-grained, FeO-poor, POP chondrule (Fig. 1e,f), in which low-Ca pyroxene phenocrysts occur in the outer regions. Chondrule 36 (Fig. 1g) has a barred olivine texture, and is the only FeO-rich chondrule studied (mean Fa = 12 mol%). Coarse, elongated laths of olivine are typically zoned from Fa 10 at their centers to Fa 18 at their edges. Chondrule 14C (Fig. 1h) is the only Al-rich chondrule included in this study. It has a bulk Al content of 6.3 wt.% and consists of a few large (>100 μm), euhedral olivine grains and a few small (~50 μm) spinel grains in a mesostasis that consists predominantly of anorthitic plagioclase (An91). Most of the other chondrules studied have porphyritic, olivine- and pyroxene-rich textures, crystalline mesostases, and varying abundances of opaques. 13C is a compound chondrule consisting of an FeO-poor and magnetite-poor, BO inner chondrule and an FeO-poor and magnetite-rich, PO outer chondrule. For chondrule 13C, we measured two bulk oxygen analyses: both analyses could contain either or both the BO and the PO chondrules.

Although an effort was made to remove rims from chondrules by abrading them (Schilk, 1991), some fine-grained rim material and opaque rims were observed on several of the chondrules when they were examined in the SEM (e.g., Fig. 1a,e,h). Fine-grained matrix in CV chondrites has an oxygen isotope ratio that lies close to the CCAM line, and has higher $\delta^{18}O$ values (around 2‰) than most bulk chondrules (Clayton et al., 1977). In addition, some chondrules have coarse-grained rims (Rubin, 1984), e.g., chondrule 14C (Fig. 1h). Coarse-grained igneous rims around chondrules in Allende have consistently high $\delta^{18}O$ values relative to their host chondrules (Rubin et al., 1990). We did not determine whether the material we analyzed for bulk oxygen isotopes contained any rim material of any kind. We do not expect any rim material to be volumetrically significant, or to contribute significantly to the bulk chondrule measurements. For example, 5 vol.% of rim material that has a $\delta^{18}O$ value 2‰ different from the bulk chondrule will only change the $\delta^{18}O$ value of the bulk chondrule by 0.1‰.

Bulk compositions of all the chondrules studied were determined by instrumental neutron activation analysis (INAA) (Schilk, 1991; Jones and Schilk, 2000) and will be discussed in detail in a forthcoming paper. Variations in Al and Fe contents for the bulk chondrules illustrate that the chondrules for which bulk oxygen isotope ratios were measured span the range of bulk compositions of all Mokoia chondrules (Fig. 2). Bulk compositions of those chondrules for which petrology has been determined represent most of the compositional range, with the exception of the most Fe-rich bulk compositions. The chondrules for which SIMS data were obtained represent a rather

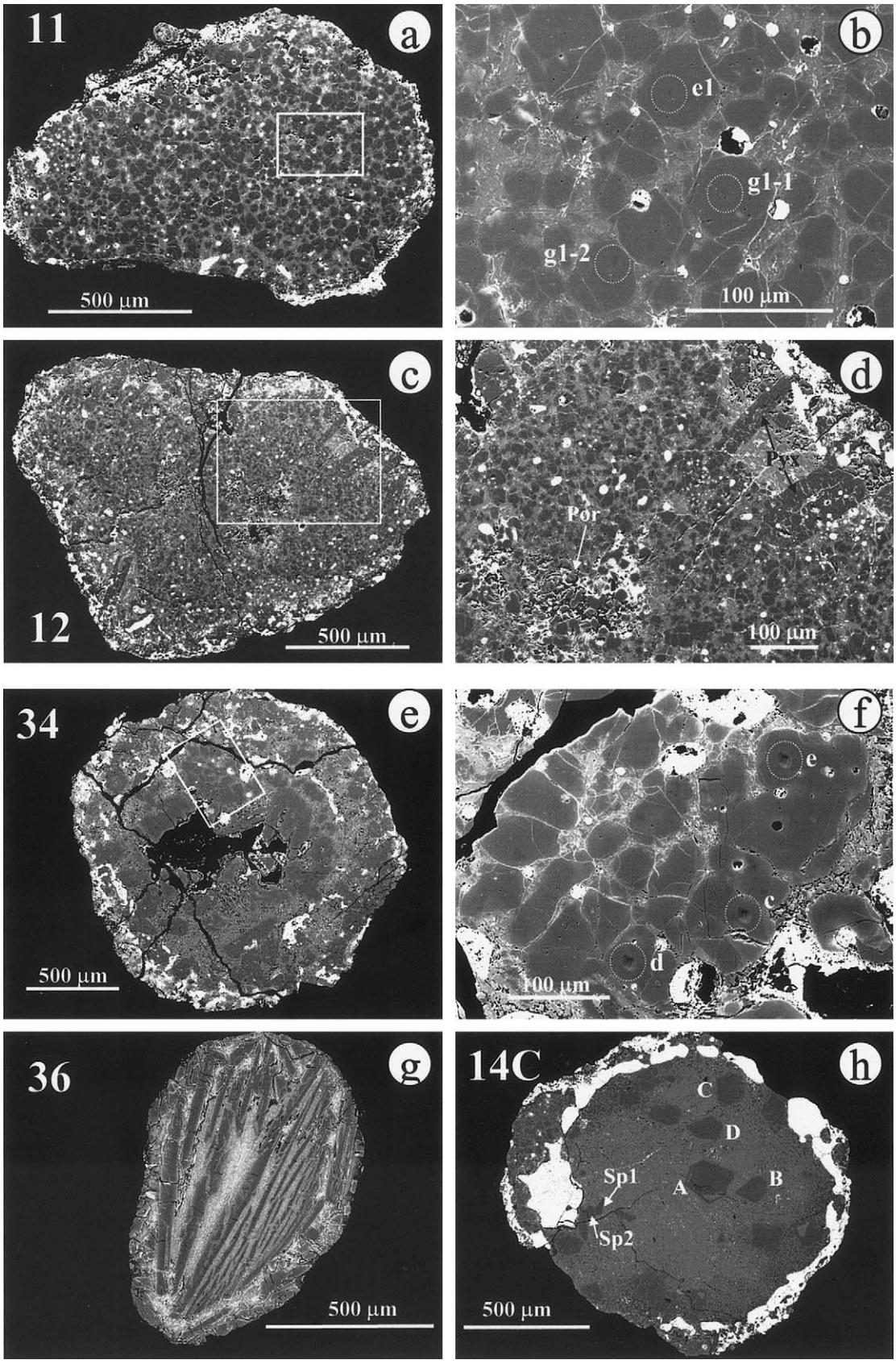
11
a
500 μm
b
e1
g1-1
g1-2
100 μm
c
12
500 μm
d
Pyx
Por
100 μm
34
e
500 μm
f
e
c
d
100 μm
36
g
500 μm
14C
h
C
D
Sp1
A
B
Sp2
500 μm

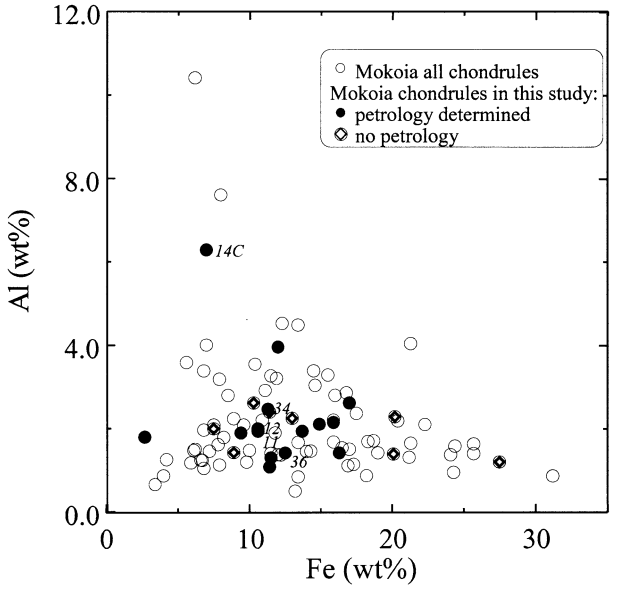

Fig. 2. Bulk chemical compositions of Mokoia chondrules (data from Schilk, 1991). The chondrules for which bulk oxygen isotope ratios were measured in this study span the range of compositions represented by all chondrules. Petrology has not been determined for the most Fe-rich chondrules. Chondrules selected for in situ analyses (labeled) represent a wide range of bulk Al, but a relatively limited range of bulk Fe.

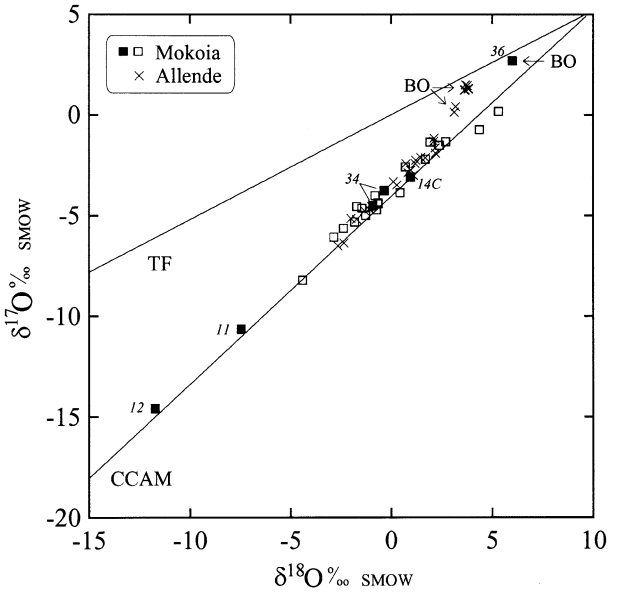

Fig. 3. Bulk oxygen isotope ratios for 23 Mokoia chondrules (see Table 1). Two analyses were obtained for chondrules 34 and 13C. Chondrules for which in situ oxygen isotope ratios were determined are shown as filled symbols: they represent the entire range of oxygen isotope ratios shown by all chondrules. Data from chondrules in the Allende chondrite (Clayton et al., 1983; Rubin et al., 1990) are shown for comparison. Mokoia chondrules show a wide range of values of $\delta^{18}O$, and define an array that lies subparallel to, but slightly above, the CCAM line. The CCAM line is defined by analyses of anhydrous minerals in CAIs from Allende (Clayton et al., 1977). TF is the terrestrial fractionation line ($\delta^{18}O = 0.52 \times \delta^{17}O$).

narrow range of bulk Fe, but a wider range of bulk Al. The one Al-rich chondrule in this study, 14C, has a bulk Al content of 6.3 wt.%. The two plagioclase-rich porphyritic chondrules, 15 and 23A (Table 1), have bulk Al contents of 2.6 and 4.0 wt.% respectively. The chondrule with the most FeO-rich olivine in this study, chondrule 36, has a bulk Fe content of 12.5 wt.%, which is in the middle of the range of the entire suite of Mokoia chondrules: the bulk Fe content of chondrules is largely a factor of the amount of iron that was originally present as metal and sulfide minerals.

Bulk oxygen isotope ratios for the chondrules studied are given in Table 1 and plotted in an oxygen three-isotope diagram in Figure 3. Most of the data form an array that lies close to, although slightly above, the CCAM line defined by anhydrous minerals in CAIs (Clayton et al., 1977). The $\delta^{18}O$ values of the Mokoia chondrules range from -11.7‰ (chondrule 12) to +5.3‰ (chondrule 36). Bulk $\delta^{18}O$ values from Allende chondrules (Clayton et al., 1983; Rubin et al., 1990) have similar values (Fig. 3).

In situ ion microprobe measurements of oxygen isotope ratios were made on individual grains in chondrules 11, 12, 34, 36 and 14C. These chondrules were selected because their bulk $\delta^{18}O$ values represent the entire range of the suite (Fig. 3), and because they represent a variety of textural types (Fig. 1). Most of the data were obtained on individual olivine grains, although two low-Ca pyroxene grains in chondrule 12, and two spinel grains in chondrule 14C, were also analyzed. The data are summarized in Table 2.

The $\delta^{18}O$ values of olivine range from −50 to +1.3‰ in chondrule 11 (Fig. 4a) and −40 to −14‰ in chondrule 12 (Fig. 4c). For both chondrules, the oxygen isotope ratios of all olivine and pyroxene grains analyzed lie on the CCAM line, within analytical error. In chondrule 12, pyroxene grains have significantly higher values of $\delta^{18}O$ than olivines (−4.6 and -1.0‰). The spatial distribution of values of $\Delta^{17}O$ for both chondrules is shown in Figures 4b and 4d. For chondrule 11, most analyses were for individual grains, although we managed to obtain two analyses on grain h2 and four analyses on the relatively large (80 × 40 μm)

Fig. 1. Back-scattered electron images of Mokoia chondrules for which in situ oxygen isotope data were obtained. (a, b) Fine-grained, PO chondrule 11: (b) is area outlined by box in (a). Circles show the positions of three oxygen isotope measurements (see Table 2). (c, d) Fine-grained, POP chondrule 12: (d) is area outlined by box in (c). In a region in the center of the chondrule, which appears to be somewhat porous ("Por"), olivine grains are enriched in FeO (lighter in the image) compared with most olivine grains in the chondrule. Low-Ca pyroxene phenocrysts (Pyx) are present in an outer region that is rich in mesostasis, and are elongated perpendicular to the outside edge of the chondrule. (e, f) PO chondrule 34: (f) is area outlined by box in (e). Circles show the positions of three oxygen isotope measurements (see Table 2). (g) FeO-rich, BO chondrule 36; (h) Al-rich chondrule 14C, which includes large olivine grains (oxygen isotope analyses were obtained on grains labeled A-D), small spinel grains (e.g., Sp1 and Sp2), a high proportion of plagioclase-rich mesostasis, and an opaque-rich rim.

Table 2. Oxygen isotope ratios (SIMS analyses) of individual olivine and pyroxene grains in Mokoia chondrules.

Mineral	Grain	Analysis	$\delta^{18}O$ (‰)	2σ	$\delta^{17}O$ (‰)	2σ	$\Delta^{17}O$ (‰)
Chondrule 11							
olivine	e1		−18.0	4.7	−22.2	3.0	−12.8
olivine	f1	a	−41.3	4.5	−43.9	3.1	−22.4
olivine	f1	b	−50.2	3.2	−48.9	2.5	−22.8
olivine	f1	d1	−49.8	1.8	−46.7	2.0	−20.8
olivine	f1	d2	−51.3	1.9	−47.5	2.2	−20.8
olivine	f2		−14.2	3.2	−14.3	2.5	−6.9
olivine	g1-1		−46.5	2.5	−48.7	2.5	−24.6
olivine	g1-2		−41.0	1.9	−44.7	2.2	−23.4
olivine	h1		1.3	3.0	−6.2	2.3	−6.9
olivine	h2	a	−11.6	3.1	−12.3	2.5	−6.3
olivine	h2	b	−4.2	2.0	−6.9	2.1	−4.7
olivine	j1		−33.5	3.2	−33.4	2.5	−15.9
olivine	k1		−13.2	3.2	−13.0	2.6	−6.1
olivine	m1		−45.2	1.9	−45.8	2.3	−22.3
olivine	m2		−17.3	3.2	−16.5	2.4	−7.5
olivine	o1		−34.5	3.2	−36.3	2.5	−18.3
Chondrule 12							
olivine	b1d		−27.9	5.1	−30.7	3.0	−16.2
olivine	b3c		−14.5	5.1	−23.7	3.0	−16.2
olivine	b4e		−22.0	5.1	−25.6	2.9	−14.2
olivine	b2d		−16.7	5.1	−20.6	3.0	−11.9
olivine	b3a		−19.2	5.1	−25.7	3.0	−15.7
olivine	b2c-1		−32.0	1.5	−31.9	2.2	−15.3
olivine	b2c-2		−39.4	1.4	−39.5	2.2	−19.0
olivine	b2c-3		−40.0	1.6	−39.9	1.9	−19.1
olivine	b2c-4		−23.8	1.6	−30.8	2.1	−18.4
olivine	b2c-5		−32.4	1.9	−34.4	2.2	−17.6
olivine	b4d-1		−26.0	2.3	−27.4	2.2	−13.9
olivine	b4d-2		−25.2	1.7	−26.7	2.3	−13.6
pyroxene	b1eepyx		−4.6	1.7	−7.9	2.4	−5.5
pyroxene	b3apyx		−1.0	5.1	−5.2	3.1	−4.6
Chondrule 34							
olivine	A		−3.8	2.5	−6.9	3.3	−4.9
olivine	B		−3.6	2.5	−7.9	3.4	−6.0
olivine	C		−8.1	2.4	−11.2	3.3	−7.0
olivine	D		0.4	2.6	−4.2	3.7	−4.4
olivine	E		1.3	2.7	−4.1	3.2	−4.7
Chondrule 36							
olivine	1b		12.7	3.7	4.9	3.2	−1.7
olivine	2b		5.0	3.7	0.9	3.2	−1.7
olivine	4b		12.2	3.7	7.0	3.4	0.6
Chondrule 14C							
olivine	A	core1	−15.7	3.3	−14.2	3.6	−6.0
olivine	A	core2	−4.2	4.0	−9.2	4.2	−7.0
olivine	A	rim1	−5.2	3.5	−10.0	3.7	−7.3
olivine	A	rim2	−5.0	3.3	−8.7	3.7	−6.1
olivine	B	core	−6.2	3.0	−8.6	3.7	−5.4
olivine	C	core	−4.9	3.7	−10.2	3.6	−7.7
olivine	C	rim	−10.0	3.1	−13.4	3.8	−8.2
olivine	D	core	−4.1	3.4	−9.9	3.7	−7.8
olivine	D	rim	−8.5	3.2	−12.9	3.7	−8.5
spinel	Sp1		−6.6	3.2	−9.4	3.9	−6.0
spinel	Sp2		−5.1	3.6	−9.4	3.9	−6.8

grain f1, which appears to be a single crystal (Fig. 5a). Both grains were, isotopically, relatively homogeneous, one being among the most ^{16}O-rich and the other the least ^{16}O-rich (Table 2; Fig. 4a,b). Olivine grains in chondrule 12 were too small for more than one analysis on each grain. Analyses of olivine in the central, porous region of chondrule 12 tended to have lowest $\delta^{18}O$ values of -18 to -19‰ (Fig. 4c,d).

Figure 6 shows the variation in minor element compositions between olivine grains in chondrules 11 and 12, as a function of $\Delta^{17}O$ values. For several of the grains, the composition given is the mean of several analyses obtained in a zoning profile that was made across the grain before the SIMS measurement was made. Other compositions are for as few as one electron microprobe analysis per grain. Most grains were very homogeneous and show little or no zoning in major or minor elements, as illustrated in Figure 5b, which shows a compositional profile across grain f1 in chondrule 11. Figure 6 shows that olivine in both chondrules is rather homogeneous and shows little variation in minor element compositions from grain to grain. There are no correlations between minor element

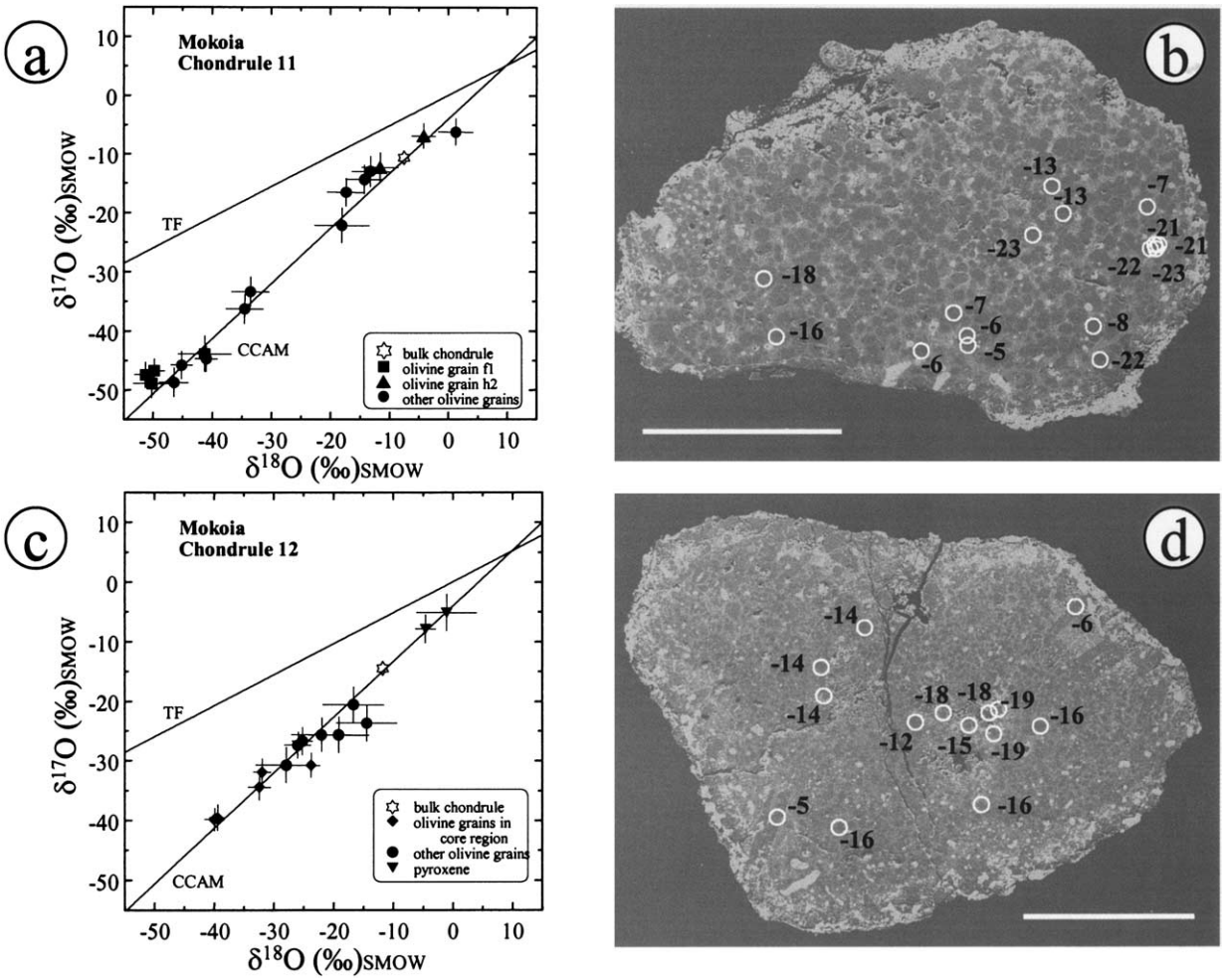

Fig. 4. Oxygen isotope ratios of individual olivine and pyroxene grains in Mokoia chondrules 11 (a) and 12 (c), and the spatial distribution of values of $\Delta^{17}O$ (‰) within these chondrules (b, d). Oxygen isotope ratios in both chondrules are extremely heterogeneous. There are no apparent relationships between spatial locations of the grains and their oxygen isotope ratios. In both chondrules, $\delta^{18}O$ values of most olivine grains are lower than those of the bulk chondrules (open star symbols). Low-Ca pyroxene in chondrule 12 has lower values of $\Delta^{17}O$ than olivine. Scale bars are 500 μm.

concentrations and $\Delta^{17}O$ values, except for a weak correlation for FeO in chondrule 12. FeO-rich olivine, from the central, porous region in chondrule 12, has relatively low $\Delta^{17}O$ values compared with olivine in the un-metamorphosed main part of the chondrule. However, low $\Delta^{17}O$ values are not restricted to this porous zone, as can be seen in Figure 4d, and variations in $\Delta^{17}O$ show no obvious spatial relationship to the edge of the chondrule or the porous zone.

For chondrules 34, 36, and 14C, we measured oxygen isotope ratios in situ on a limited number of olivine grains. The data are summarized in Figure 7. In all these chondrules, analyses of olivine are distributed along the CCAM line, as is the case for chondrules 11 and 12, although olivine grains in 34, 36, and 14C are distributed across a much more restricted range than we observed in chondrules 11 and 12. In chondrule 14C, olivine has lower $\delta^{18}O$ values than the host bulk chondrule, whereas in chondrule 34, olivine has slightly lower $\delta^{18}O$ values than the bulk, and in chondrule 36, olivine has slightly higher $\delta^{18}O$ values than the bulk. The difference between the olivines and the bulk in 14C is consistent with this chondrule having a high proportion of mesostasis (Fig. 1g), which must have higher $\delta^{18}O$ values than the olivine.

For chondrule 14C, we obtained analyses from the cores and rims of the largest olivine grains (Fig. 8a). These grains show zoning in cathodoluminescence (Fig. 8b), with the intensity decreasing monotonically from core to rim. The grains are weakly and normally zoned in FeO and MgO, and show zoning of minor elements, including decreases in CaO and Al_2O_3, and an increase in Cr_2O_3, from core to rim (Fig. 8c). Within the errors of our measurements, there is no distinguishable difference in oxygen isotope ratios between the cores and rims of these olivine grains (Fig. 7c). Oxygen isotope ratios of spinel grains in this chondrule are indistinguishable from the olivine data.

4. DISCUSSION

4.1. Bulk Chondrule Oxygen Isotope Ratios

4.1.1. Comparison with Allende and possible secondary effects

Our data for bulk oxygen isotope ratios of Mokoia chondrules show general similarities to previous data obtained for

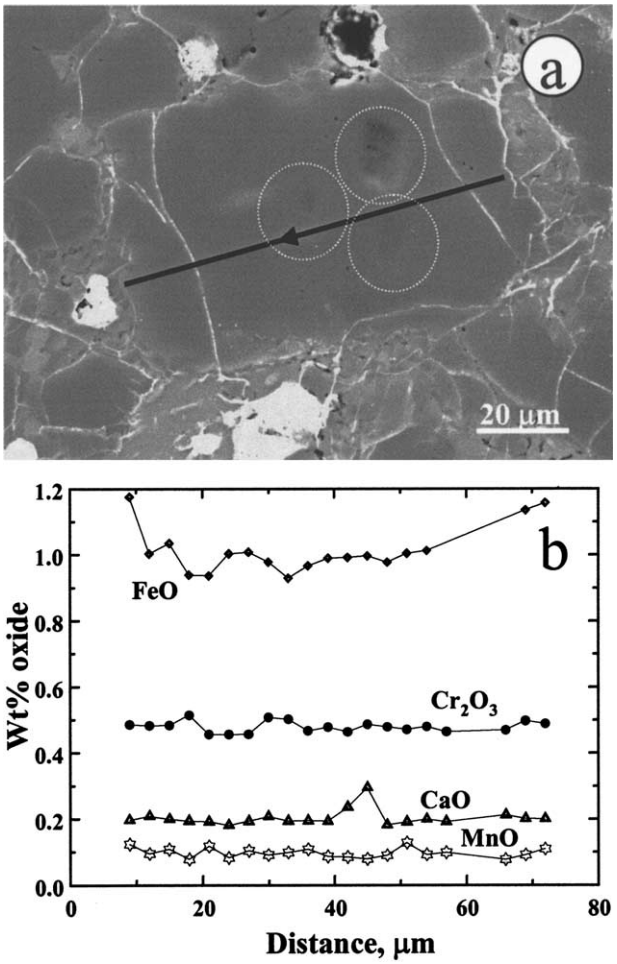

Fig. 5. Grain f1 in chondrule 11, the grain on which we obtained four oxygen isotope analyses. (a) Back-scattered electron image of grain f1 after SIMS analysis, showing the location of the analysis pits. Two of the analyses (d1, d2) were obtained consecutively on the same (uppermost) spot. The arrow shows the position and direction of the electron microprobe traverse, shown in (b), that was obtained before SIMS analyses. Light gray streaks are an artifact of the SIMS analyses.

chondrules from Allende (Clayton et al., 1983; Rubin et al., 1990): they mostly form an array that lies parallel to, but slightly higher than, the CCAM line on an oxygen three-isotope plot (Fig. 3). Thus, it is clear that the (oxidized) CV chondrule suite in general, rather than the Allende suite in particular, shows these general properties. Despite the general similarities between the Mokoia and Allende data sets, it is important to discuss some salient differences, which may serve to shed additional light on important aspects of the chondrule formation process.

Our data for Mokoia show a significantly wider spread than any set of bulk chondrules measured previously. The most ^{16}O-rich chondrule measured previously in Allende had a δ^{18}O value of -2.7‰. The extension of the data array by more than 10‰ in δ^{18}O has important implications, not the least of which is that it shows that the data for CV chondrules do in fact lie on an array that is subparallel to the CCAM line. This interpretation was somewhat ambiguous for the Allende data, because of the apparent upswing in the trend towards the terrestrial fractionation (TF) line at the ^{16}O-poor end of the array. The Allende chondrules that lie close to the TF line are FeO-rich, BO chondrules (Clayton et al., 1983; McSween, 1985). From the Allende data it was not clear whether CV chondrules form a single, continuous array with a steep slope, or whether the FeO-rich chondrules have undergone secondary exchange from an initial array with a slope close to one. Our data suggest that the latter interpretation is more likely correct. The only FeO-rich, BO chondrule that we analyzed (chondrule 36) lies in a position that could be interpreted either as an extension of the main CV chondrule array, or as a part of the same FeO-rich, BO group as those in Allende.

The Allende chondrite has been subjected to a complex alteration history, probably involving aqueous alteration and subsequent dehydration that took place on its parent body after accretion (Krot et al., 1995). Fayalite-rich rims on forsterite grains in porphyritic olivine chondrules in Allende (Peck and Wood, 1987; Hua et al., 1988) probably result from this complex processing. We observe no comparable fayalite-rich rims on forsterite grains in the Mokoia chondrules included in this study. Oxygen isotope ratios in the Mokoia chondrule suite are therefore more likely to be representative of primary nebular properties than those in the Allende suite. However, any differences in secondary processing do not appear to have had a significant effect on bulk chondrule oxygen isotope ratios, because the data for Allende and Mokoia are essentially indistinguishable. Some of the Mokoia chondrules in our study show the effects of mild metamorphism, but this apparently also has only a negligible effect on the oxygen isotope ratios of the bulk chondrules. The three chondrules that show the most significant effects of metamorphism (33, 24A, 5C) do not depart significantly from the main array of data in Figure 3.

Both Mokoia and Allende are oxidized CV chondrites, in which Fe,Ni metal that was originally present has been oxidized to magnetite, probably in an asteroidal setting after accretion (Housley and Cirlin, 1983; Krot et al., 1995; Choi et al., 1997, 2000). Most of the Mokoia chondrules studied contain at least some magnetite, although chondrules 12C and 36 do not contain any. Choi et al. (2000) showed that magnetite in Mokoia has a lower Δ^{17}O value than forsteritic olivine, with a Δ^{17}O value of about −1‰ and δ^{18}O of ~3‰. The contribution of magnetite to the bulk chondrule oxygen isotope ratio may be significant for opaque-rich chondrules, and cause the bulk data to be displaced towards lower Δ^{17}O values relative to the original chondrule material. We have not determined proportions of magnetite in each chondrule in this study, so we have not evaluated the possible effect of magnetite on the bulk data quantitatively. However, because the bulk data for chondrule 12C, which contains no magnetite, and chondrule 14C, which contains a significant amount of magnetite in an opaque rim (Fig. 1h), both lie close to the CCAM line, the effect does not appear to be noticeable within our data set.

Oxygen isotope ratios for two chondrules from Mokoia, the plagioclase-rich POP chondrule 23A, and chondrule 80, the petrology of which was not determined, lie slightly below the CCAM line. These chondrules lie close to the slope 0.5, Allende mass fractionation (AMF) line (Fig. 9). Chondrule 23A does not show any strong evidence for extensive alteration in the form of Na metasomatism or aqueous alteration, such as that observed in Allende CAIs and chondrules (Young and

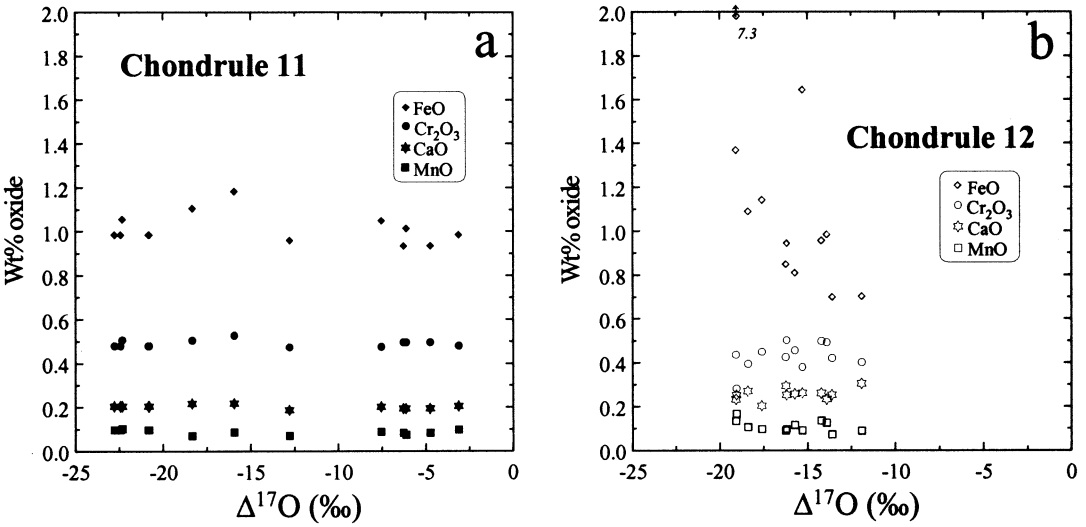

Fig. 6. Variation in $\Delta^{17}O$ (‰) in chondrules 11 and 12, as a function of the chemical compositions of individual olivine grains. In chondrule 11, and for most elements in chondrule 12, there is no correlation between $\Delta^{17}O$ and chemistry. FeO contents of olivine grains in chondrule 12 show a negative correlation with $\Delta^{17}O$.

Russell, 1998; Ash and Young, 2000; Young et al., 2002). Bulk Na contents of both 23A (0.43 wt.%) and 80 (0.37 wt.%) are very typical of the entire ferromagnesian chondrule suite in Mokoia (Schilk, 1991), and the plagioclase in chondrule 23A has a composition of An_{96}. Young and Russell (1998) also suggested that the melilite mass fractionation line could be the result of evaporative processes that did not necessarily include Na reactions. It is possible that chondrules 23A and 80 are part of such a trend, and that fractionation occurred during evaporation of either plagioclase or a melt.

To summarize, even though Allende and, to a lesser extent, Mokoia, have been altered by secondary processing, there are essentially no manifestations of these effects in the bulk oxygen isotope ratios of most chondrules. The most significant effects appear to be present in chondrules with high $\delta^{18}O$ in which there is greater dispersion about the CCAM line.

4.1.2. Isotopic evolution of CV chondrite components

The distribution of oxygen isotope ratios in bulk CAIs from Allende is controlled by the fact that individual mineral separates have oxygen isotope ratios that vary along the CCAM line ($\delta^{17}O = 0.94 \times \delta^{18}O - 4.1$: Clayton et al., 1977). The CCAM line has generally been considered to describe the behavior of most materials in CV chondrites, including bulk chondrule data for Allende chondrules that have been shown to lie slightly above this line (Clayton et al., 1983; Rubin et al., 1990: Fig. 3). However, Young and Russell (1998) defined a different line, with a slope of 1.00 ($\delta^{17}O = 1.00 \times \delta^{18}O - 1.044$), based on high-precision, in situ analyses of unaltered minerals in a single CAI from Allende (The Y&R line: Figs. 9 and 10). This line converges with CCAM at $\delta^{18}O$ values around -40‰, corresponding to oxygen isotopic compositions of spinels in CAIs, and intersects with oxygen isotopic compositions of ordinary chondrites at the low-^{16}O end. Young and Russell (1998) described this line as the "primitive oxygen isotope reservoir" of the early solar nebula. They interpret the CCAM line as resulting from mass fractionation at the ^{16}O-poor end of the Y&R line during secondary alteration processes of CAI minerals, along the AMF line (Fig. 9).

Several different scenarios have been proposed to account for a distribution of oxygen isotope ratios along a line of slope one: (1) Oxygen isotope exchange between initially ^{16}O-rich CAI minerals with $\delta^{18}O$ around -40‰, and an ^{16}O-poor nebula gas with $\delta^{18}O$ around 0‰ (Clayton, 1993); (2) Non-mass-dependent fractionation processes in the solar nebula (Thiemens, 1996); (3) Isotopic self-shielding either in the solar nebula or in the molecular cloud from which the solar nebula formed (Clayton, 2002; Yurimoto and Kuramoto, 2002; Lyons and Young, 2003). Different models predict different values for the bulk solar oxygen isotopic composition (Wiens et al., 1999).

Despite considerable discussion of the nature of the Y&R line and its relationship to CCAM, few papers have considered in detail how the oxygen isotope ratios for bulk chondrules may be accounted for in terms of either of these proposed arrays. The exact slope of the array defined by the CV chondrule data is somewhat ambiguous because of uncertainties in the cause of the dispersion of data at the ^{16}O-poor end of the array. A best-fit line to all the CV chondrule data (Allende and Mokoia combined) has a slope of 0.99 ($\delta^{17}O = 0.99 \times \delta^{18}O - 3.48$: $R^2 = 0.96$). This line is plotted in Figure 9. However, if we exclude the Mokoia and Allende data for FeO-rich BO chondrules, plus the Mokoia data that lie below the CCAM line (i.e., chondrules with $\delta^{18}O > 3‰$), the best-fit line has a slope of 0.94, and is essentially coincident with the CCAM line ($\delta^{17}O = 0.94 \times \delta^{18}O - 3.61$: $R^2 = 0.98$). Although it is possible that all of the chondrules with $\delta^{18}O > 3‰$ have been affected by secondary processes, particularly the FeO-rich BO chondrules from Allende, no substantial arguments have been put forward for this possibility, and we prefer at this point to use the slope-0.99 line as the one that defines the entire CV chondrule array. This line (CV-ch, Figs. 9 and 10) is displaced signifi-

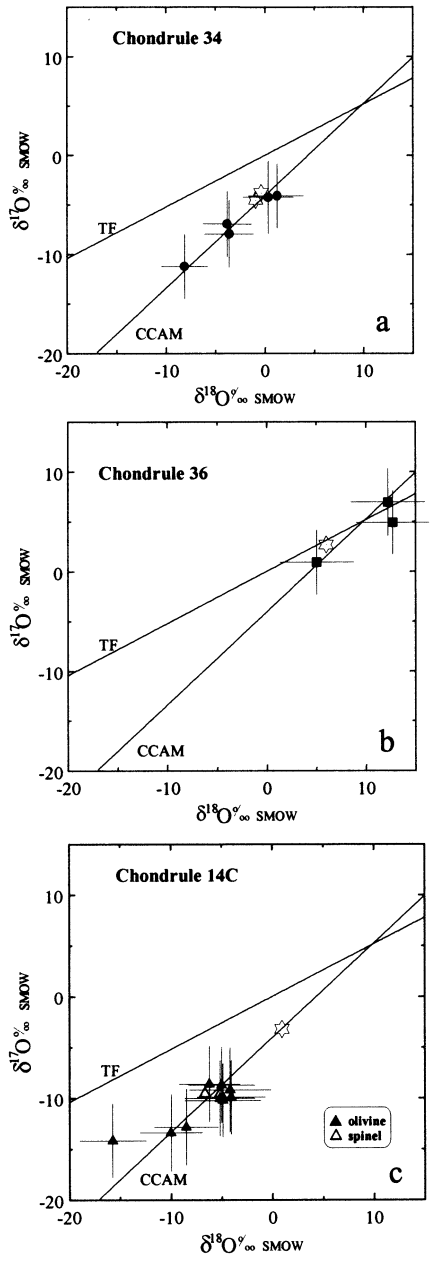

Fig. 7. Oxygen isotope ratios of individual olivine grains in Mokoia chondrules 34, 36, and 14C, as well as individual spinel grains in chondrule 14C. Oxygen isotope ratios in these chondrules are more homogeneous than those in chondrules 11 and 12. Bulk chondrule oxygen isotope ratios are indicated as open star symbols.

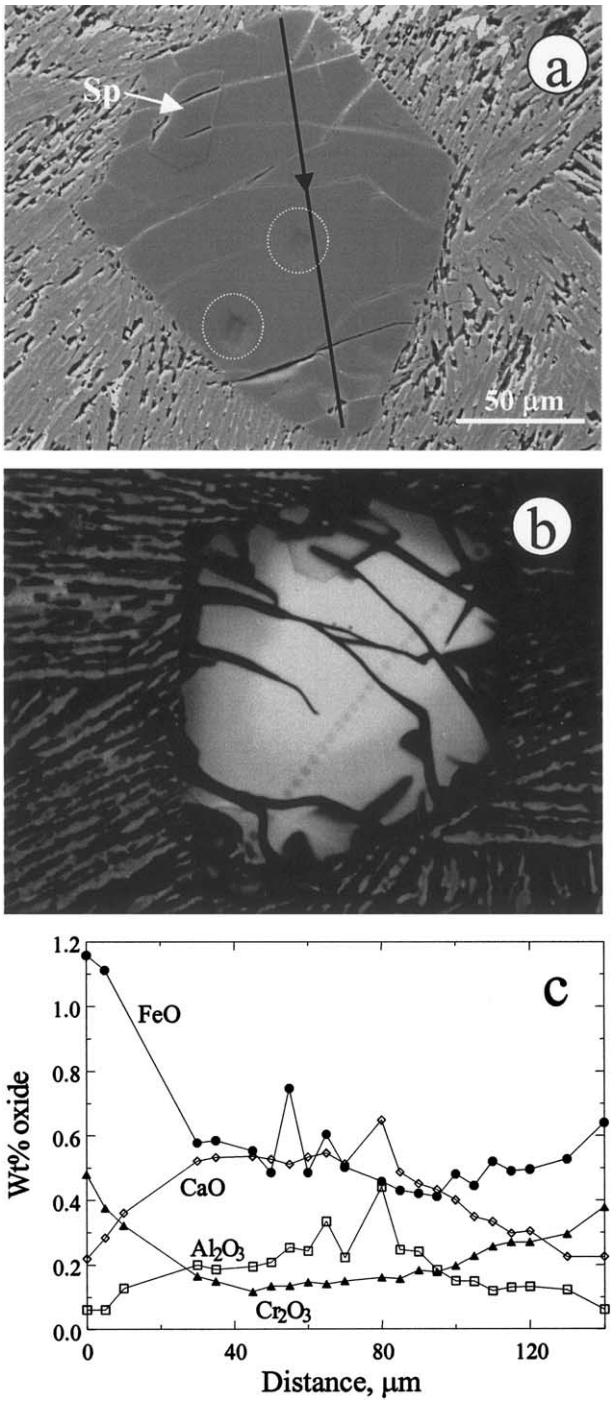

Fig. 8. Olivine grain C from chondrule 14C. (a) Back-scattered electron image. "Sp" indicates an inclusion of spinel. The arrow shows the location and direction of the electron microprobe traverse shown in (c). Circles highlight the SIMS analysis pits for this grain. (b) Cathodoluminescence (CL) image, showing that CL intensity decreases from the core to the edge of the olivine grain. The position of the electron microprobe traverse is visible as a row of spots. (c) Electron microprobe traverse showing minor element zoning across the grain. Bright CL is associated with high CaO and Al_2O_3 contents of the olivine, in the core region.

cantly from the Young and Russell line (Fig. 9), by ~2.5‰ in $\delta^{17}O$, and shows a significant departure from the CCAM line at low values of $\delta^{18}O$ (Fig. 10). The displacement of the Y&R line from CV-ch and CCAM does not appear to be the result of systematic laboratory errors, because Young and Russell (1998) and Young et al. (1998) also made several measurements of CAI phases that do lie on the CCAM line.

According to Young and Russell (1998), deviations from the Y&R line at the ^{16}O-poor end, in CAIs, are the result of secondary, mass-fractionation processes (Fig. 9). Young and Russell interpret the array of CAI data (bulk CAIs and mineral separates) that extends along the CCAM line as the result of mixing between altered CAI components and ^{16}O-rich, unal-

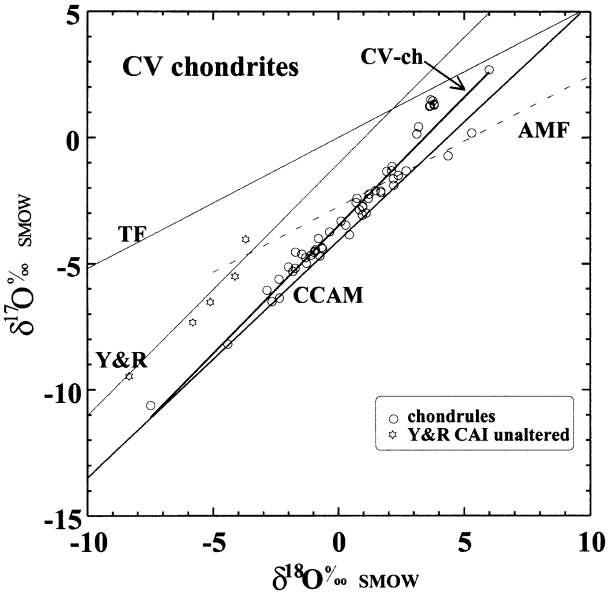

Fig. 9. Oxygen isotope ratios of bulk chondrules in the CV carbonaceous chondrites Mokoia (this study) and Allende (Clayton et al., 1983; Rubin et al., 1990), and their relationships to various defined lines on the oxygen plot. The best-fit line to all bulk chondrule data (open circles: CV-ch) has a slope of 0.99 ($r^2 = 0.96$). The Young and Russell line (Y&R), defined by high-precision analyses of unaltered minerals in a CAI from Allende (open stars: Young and Russell, 1998), has a slope of 1.00. The dashed line, AMF, is the Allende mass fractionation line (slope ~0.5, $\Delta^{17}O = -2.75‰$) that represents alteration of chondrule and CAI minerals in Allende (Young and Russell, 1988; Young et al., 2002). CCAM (see Fig. 3) has a slope of 0.94. The CV-ch line is displaced from the Y&R line by approximately 2.5‰ in $\delta^{17}O$.

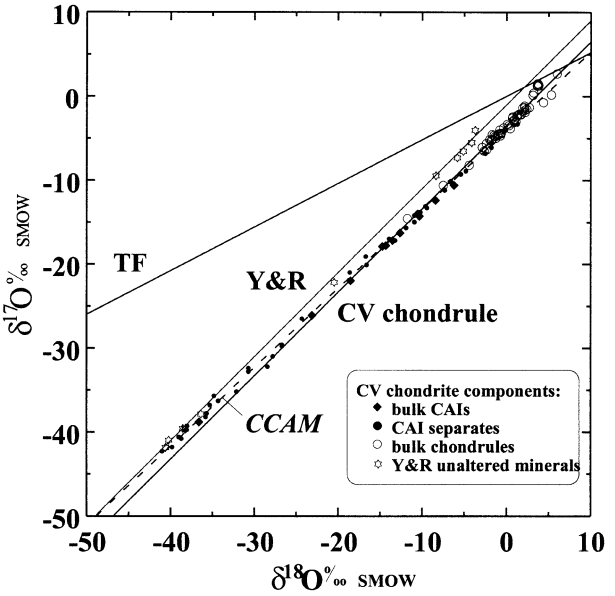

Fig. 10. High-precision data showing oxygen isotope relationships between various components in CV carbonaceous chondrites. The CV-ch, Y&R, and CCAM (dashed) lines are defined in Figure 9. The Y&R line is defined by unaltered minerals from one CAI (open stars: Young and Russell, 1998). Most bulk CAIs from Allende (filled diamonds: Clayton et al., 1977) lie on an extension of the CV-ch line. Oxygen isotope ratios for bulk chondrules and bulk CAIs overlap at values of $\delta^{18}O$ around -10‰. CAI mineral separates (filled circles) with $\delta^{18}O$ values greater than -30‰ also lie close to the CV-ch line, although more ^{16}O-rich mineral separates ($\delta^{18}O$ values around -40‰) do not.

tered spinel with $\delta^{18}O$ values around -40‰. However, the spread along the CV-ch line for chondrules cannot be interpreted in the same way as the mixing model for CAIs. Firstly, ferromagnesian chondrules do not contain an identifiable ^{16}O-rich component similar to spinel in CAIs. The ^{16}O-rich olivine data for chondrules 11 and 12 do not obviously result from the presence of relict grains (see below). Secondly, it is unlikely that all bulk chondrule data result from mass fractionation from original compositions along the Y&R line: because evidence from our in situ data show that olivine and mesostasis compositions in individual chondrules are distributed along a slope-one line (see below), the olivine and the mesostasis would have had to undergo mass fractionation independently, and would have had to fractionate to exactly the same extent in the same direction to result in the production of a second line that has a slope close to one. We suggest that the CV chondrule line is a more relevant and significant line for chondrules than the Y&R line, and we note that oxygen isotope ratios of many bulk CAIs fall along this line (Fig. 10). Also, as noted by Young and Russell (1998), not all unaltered mineral separates from CAIs fall on the Y&R line (Clayton et al., 1977; Mayeda et al., 1986; Young et al., 1998). Thus, the CV-ch line appears to be highly relevant to most of the material present in CV chondrites.

An interpretation of the relationships between the CCAM, Y&R, and CV-ch lines is essential to understanding the isotopic evolution of CV chondrite components. Oxygen isotope ratios of bulk CAIs and bulk chondrules overlap at values of $\delta^{18}O$ around -10‰. Bulk chondrules, bulk CAIs, and many CAI mineral separates fall on or close to the CV chondrule line, down to values of $\delta^{18}O$ around -30‰ (Fig. 10). For $\delta^{18}O$ values between -30 and -50‰, most CV components lie closer to the Y&R line than to the CV-ch line. Since we are unable to determine whether the best-fit line for chondrules should have a slope more similar to the CCAM line (0.94), because of uncertainties in the ^{16}O-poor data (see above), the relationship between ^{16}O-rich CAIs and chondrules is not completely clear. Although data for one CAI fall along the Y&R line (Young and Russell, 1998), it appears that most CAIs form a continuous array with bulk chondrules and chondrule components. Hence, there is a close association between the oxygen isotope reservoirs (solids and/or gases) from which many CAIs and all chondrules formed, and the processes of oxygen isotopic evolution that they or their precursors underwent. This conclusion is supported by observations of physical associations between CAIs and chondrules (e.g., Itoh and Yurimoto, 2003). Several authors (e.g., McKeegan et al., 1998; Wasson, 2000; Krot et al., 2002) have suggested that CAIs formed in a different isotopic environment from chondrules, for example that CAIs were formed close to the protosun in an X-wind environment (Shu et al., 1996). However, even if independent formation processes are invoked, fundamental relationships between the oxygen isotope ratios of CAIs and chondrules (at least for the oxidized CV chondrites) show these two components to be intimately associated.

4.2. In situ Oxygen Isotope Data

The five chondrules that we selected for in situ oxygen isotope analyses span the entire range of $\delta^{18}O$ values for the Mokoia suite (Fig. 3), and represent a range of textural and compositional types (Fig. 1). Several general observations can be made about our SIMS data. First, oxygen isotope ratios of olivine grains are extremely variable, demonstrating that the array of oxygen isotope ratios shown by bulk chondrules is not the result of simple mixing of two endmembers, such as olivine and mesostasis. Second, oxygen isotope ratios of the olivine grains tend to correlate with the bulk oxygen isotope ratios measured (Figs. 4 and 7): for example, the chondrules with the lowest bulk $\delta^{18}O$ values (11 and 12) are those in which the most ^{16}O-rich olivine grains are observed, and the chondrule with the highest bulk $\delta^{18}O$ value (36) is the one that contains the most ^{16}O-rich olivine grains. Third, in general, we infer that chondrule mesostases are depleted in ^{16}O relative to the bulks: in chondrules 11, 12, 34, and 14C, most olivine grains are more ^{16}O-rich than the host bulk chondrules. Chondrule 36 differs in that olivine appears to be slightly depleted in ^{16}O relative to the bulk chondrule. Such isotopic differences between different phases in the same chondrules could be the result of partial exchange of oxygen with a gas during chondrule formation, or exchange of oxygen in the solid state either before or after the chondrite accreted. These possibilities are discussed further below.

4.2.1. Microporphyritic chondrules, 11 and 12

Chondrules 11 and 12 have bulk oxygen isotope ratios that are notably enriched in ^{16}O relative to the main group, with $\delta^{18}O$ values of -7.5 and -11.7‰ respectively (Table 1, Fig. 3). In situ analyses of individual olivine grains in both of these chondrules show remarkable heterogeneity (Fig. 4), with a range of $\delta^{18}O$ values of ~50‰ in chondrule 11 and 30‰ in chondrule 12. There are very few known examples of olivine grains in ferromagnesian chondrules that show enrichments in ^{16}O equivalent to values of $\delta^{18}O$ around -50‰ (e.g., Yurimoto and Wasson, 2002), and this is the first reported example of such extreme isotopic heterogeneity in chondrules in which there are no obvious differences in chemical composition or texture between the grains. (The ^{16}O-rich forsterite observed by Yurimoto and Wasson (2002) within a type II chondrule in the CO3 chondrite, Yamato 81020, was interpreted as having recrystallized from a melt in which a relict AOA was locally incorporated.) The isotopic heterogeneity in chondrules 11 and 12 appears to be predominantly grain-to-grain heterogeneity, and in most cases does not appear to be correlated with the spatial location of the grain within the chondrule (Fig. 4b,d). In chondrule 12, large negative values of $\Delta^{17}O$ (-15 to -19‰) are associated with olivine in the central, porous, region, but enrichments in ^{16}O are not restricted to this region.

Within CAIs in CV chondrites, oxygen isotopic heterogeneity on a similar scale, and with an array of similar slope to that observed in chondrules (the CCAM line or the Y&R line: see above) has been attributed to solid-state exchange of oxygen between an initially ^{16}O-rich CAI and an external reservoir (such as the nebular gas), after solidification of the CAI (Clayton, 1993). A solid-state mechanism was also proposed by Bridges et al. (1999) to account for the oxygen isotope distribution observed in chondrules from partially equilibrated ordinary chondrites that have undergone metamorphism at low temperatures. In both these cases, the spread in the data is mineral-specific, and reflects different diffusion rates of oxygen in the constituent minerals. However, for chondrules 11 and 12, we cannot invoke such a mechanism to explain the spread in the data, because the spread occurs within a single mineral phase, olivine, and because there appears to be no spatial relationship such as a relationship between $\Delta^{17}O$ and distance from the edge of the chondrule (Fig. 4). Thus we discount postsolidification diffusion as a reasonable mechanism to introduce isotopic heterogeneity into the chondrules, either in the nebula or in the parent body after accretion. We consider two possibilities for the origin of the isotopic heterogeneity in chondrules 11 and 12: 1) that relict, ^{16}O-rich grains are present, and 2) that isotopic heterogeneity is the result of partial exchange between melt and gas during chondrule formation.

In the case of incorporation of ^{16}O-rich relict grains into the host chondrules, ^{16}O-rich olivine would be incorporated into the precursor assemblage, and would not melt during chondrule formation. Jones et al. (2000) showed that relict forsterite in a type II chondrule from the CO3 chondrite, ALHA77307, retained its oxygen isotope signature during formation of the host chondrule. For a relict-grain scenario, an array with a slope of one could represent solid-solid mixing, in which the solid chondrule precursors contained both ^{16}O-rich and ^{16}O-poor materials. Solid material rich in^{16}O (with $\delta^{18}O$ values around -50‰) may be derived from refractory inclusions such as CAIs or AOAs, whereas ^{16}O-poor solid material (with $\delta^{18}O$ values around 10‰) may be characteristic of solids that condensed in the chondrule-forming region. Although oxygen isotope ratios for CAIs in CV chondrites only go down to $\delta^{18}O$ values around -40‰, CAIs and AOAs in other chondrite groups, such as the CM chondrites, do extend to values of $\delta^{18}O$ around -50‰ (Hiyagon and Hashimoto, 1999). (The most extreme ^{16}O enrichment reported to date in chondritic material is a value of $\delta^{18}O$ around -75‰ in a cryptocrystalline chondrule with an olivine shell, from the Acfer 214 CH chondrite; Kobayashi et al., 2003).

Texturally and chemically, chondrules 11 and 12 are unremarkable in that they appear to be very typical type IA, PO, ferromagnesian chondrules. Their bulk chemical compositions are very similar to each other, and indistinguishable from bulk compositions of the majority of ferromagnesian chondrules in the Mokoia suite studied (e.g., Fig. 2; see also Schilk, 1991). From studies of experimental analogs, it appears that to produce a microporphyritic texture, nucleation sites that are essentially the remnants of precursor solid grains must remain in the melt during chondrule formation (Lofgren, 1996). The question that needs to be addressed for chondrules 11 and 12 is whether the olivine grains present grew from a chondrule melt (i.e., the relict-grain nucleation sites were microscopic, and are no longer identifiable, at least at the resolution of the SEM) or whether a large percentage of the volume of the olivine grains present is relict material. Lofgren (2000) has argued that a large proportion of the olivine grains present are relicts, and that only a narrow overgrowth on each grain grew from the chondrule melt.

In chondrule 12, the outer zone in which low-pyroxene grains are arranged perpendicular to the chondrule rims, and in which a high proportion of mesostasis is present, suggests

growth of the low-Ca pyroxene, at least, from a melt. However, it is possible that the olivine grains throughout the chondrule are relicts. In both chondrules 11 and 12 there is no indication, either from composition or texture, that enrichments in ^{16}O are associated with grains that may be relicts. Olivine grains in both chondrules are chemically homogeneous, showing essentially no zoning from cores to rims of individual grains, and little compositional variation from grain to grain (Figs. 5 and 6). The most obvious plausible source of ^{16}O-rich relict forsterite is AOAs. However, although forsterite grains in AOAs in CV chondrites have similar FeO contents to olivine in chondrules 11 and 12 (0.4-2 wt.%: Komatsu et al., 2001), they also contain abundant pores and tiny inclusions of Al-diopside (Komatsu et al., 2001), neither of which is observed in chondrules 11 and 12, and they contain <0.1 wt.% Cr_2O_3 and MnO (Komatsu et al., 2001), compared with levels around 0.4-0.5 wt.% Cr_2O_3 and ~ 0.1 wt.% MnO in chondrules 11 and 12. Thus, olivine in chondrules 11 and 12 is not direct relict AOA material. Olivine from the central, porous, region of chondrule 12 shows some enrichment in FeO that appears to be the result of minor, secondary, metamorphism. Minor elements (Cr_2O_3, CaO and MnO) have not been affected greatly by this process. There is essentially no correlation between oxygen isotope ratios and olivine chemistry (Fig. 6), and there are no compelling compositional arguments that the ^{16}O-rich olivine grains in chondrules 11 and 12 are relict grains. If relict grains were present originally, they either had the same chemical compositions as the chondrule olivine that grew from the melt, which we consider unlikely, or the chemical evidence that they are relicts has been eradicated by secondary, solid-state diffusion.

It is possible that olivine grains may have been homogenized chemically while retaining oxygen isotope heterogeneities, because, for volume diffusion in the solid state, diffusion of oxygen in olivine is considerably slower than cation diffusion (Freer, 1990). Chemical homogenization of relict grains could plausibly have taken place at high temperature, during chondrule formation. The diffusion coefficient of Ca^{2+} cations in olivine is around 10^{-10} cm^2 s^{-1} at 1550°C (Morioka, 1981). Using the relationship $x^2 = Dt$, diffusion of Ca over 10 μm would take ~ 3 h at this temperature. Calcium ions diffuse more slowly than the other measured cations (Fe, Mg, Mn, and Cr), and 1550°C is a minimum peak temperature for chondrule formation (Hewins and Connolly, 1996). For MgO-rich chondrules like chondrules 11 and 12, peak temperatures may have been closer to 1900°C (Hewins and Connolly, 1996), at which temperature diffusion would have been much faster. Thus, it is reasonable that olivine in chondrules 11 and 12 could have been homogenized chemically by solid-state diffusion during chondrule formation. In contrast, oxygen isotopic heterogeneity could have been preserved under the same conditions. At 1550°C, and at an oxygen fugacity corresponding to the iron-wüstite buffer, the diffusion coefficient of oxygen in forsterite is $\sim 10^{-14}$ cm^2 s^{-1} (Ryerson et al., 1989). Oxygen diffusion over 10 μm at this temperature would take ~ 3 yr.

If isotopic heterogeneity resulted from solid-solid mixing, then it follows that ^{16}O-rich solid material was a ubiquitous component of chondrule precursor material (in CV carbonaceous chondrites), resulting in the oxygen isotope ratios of all bulk chondrules falling along the same mixing line (the CV-ch line, Fig. 10).

An alternative to the above model is that the spread in oxygen isotope ratios results from interactions between solid and gas reservoirs with different abundances of ^{16}O during chondrule formation, for example between a chondrule that is ^{16}O-rich, and an ^{16}O-poor gas. Gas/melt exchange has been proposed previously to explain oxygen isotope data for CAIs (Clayton, 1993), ferromagnesian chondrules (McSween, 1985), and aluminum-rich chondrules (Russell et al., 2000). Exchange could occur during chondrule formation, when the chondrule was molten. In this scenario, the precursors to chondrules 11 and 12 had $\delta^{18}O$ values around -50‰. The first olivine grains to grow from the molten chondrule were ^{16}O-rich. Oxygen isotope exchange with a ^{16}O-poor nebula gas occurred rapidly as the chondrule cooled, so that olivine grains that nucleated and grew successively reflected the isotopic ratio of the progressively more ^{16}O-depleted melt. Oxygen isotope exchange between gas and melt has been shown experimentally to occur on short time scales (minutes) at chondrule formation temperatures (Yu et al., 1995).

The observation that low-Ca pyroxene grains in the outer zone of chondrule 12 are more depleted in ^{16}O than the olivines in the chondrule interior is consistent with a gas/melt exchange model. A high abundance of pyroxene at the edge of a chondrule has been suggested to be the result of silicon condensation during chondrule formation (Tissandier et al., 2002), which might have accompanied oxygen exchange. Inferred depletions in ^{16}O in mesostasis relative to olivine in the same chondrule (see above) would also be consistent with this model. The observations that low-Ca pyroxene in chondrule 12, and mesostasis in general in all chondrules, have lower ^{16}O than olivine argue against the possibility that the solid was ^{16}O-poor and the gas was ^{16}O-rich.

If oxygen isotope heterogeneity is the result of isotopic exchange between an ^{16}O-rich chondrule melt and an ^{16}O-poor nebular gas, this has important implications for understanding the distribution of oxygen isotopes in the solar nebula. It raises the possibility that the precursors of ferromagnesian chondrules (i.e., most of the solid material forming in the solar nebula) had initial oxygen isotope ratios corresponding to $\delta^{17}O$, $\delta^{18}O$ values around -50‰. Clayton and Mayeda (1984) proposed that oxygen isotope ratios of chondrule precursors could have initially been as ^{16}O-rich as refractory inclusions, on the basis of observations on CM chondrites. Clayton (2002) also argued that this was the case, based on an isotopic self-shielding model. It is possible that chondrules 11 and 12 represent the first generation of chondrules, i.e., the first batch of material that underwent chondrule formation. Subsequent recycling of chondrule material and equilibration with nebular gas may have resulted in the grouping of oxygen isotope ratios of bulk chondrules in carbonaceous chondrites around $\delta^{18}O$ values ≈ 0‰. The differences in oxygen isotope ratios between chondrules and CAIs may be attributable to a greater number of reheating events, and a greater degree of equilibration with the gas reservoir, for the chondrule population.

4.2.2. Porphyritic chondrule 34

In chondrule 34, isotopic ratios of olivine grains cluster around the mean for the bulk chondrule (Fig. 7a). In contrast to chondrules 11 and 12, the olivine data show only small varia-

tions. Although chondrule 34 is a type IA, POP chondrule, it is significantly coarser grained than chondrules 11 and 12 (Fig. 1), and the likelihood that the olivine and pyroxene grains grew from the chondrule melt is less equivocal. There are no apparent relict grains in this chondrule. According to the melt/gas exchange scenario for oxygen isotope evolution we presented above, chondrule 34 would represent the product of recycling of chondrule material in the chondrule-forming region, during which oxygen isotope ratios of the precursor solids became homogenized.

4.2.3. Barred olivine chondrule 36

As discussed above, the bulk chondrule data for chondrule 36, along with the FeO-rich barred olivine chondrules in Allende (Clayton et al., 1983: Fig. 3), could be interpreted as deviating from the general porphyritic chondrule trend that falls slightly above the CCAM line. However, if we define the CV-ch line as above (Figs. 9 and 10), the BO chondrules do not depart significantly from the main trend (Fig. 9), although since the slope of the CV-ch line is largely controlled by the data for these chondrules, this inference is partly self-fulfilling. The ion microprobe data can help to clarify the oxygen isotope relationships between barred and porphyritic chondrules: Although the errors are large, the in situ data for chondrule 36 (Fig. 7b) tend to support the interpretation that the oxygen isotope composition of this chondrule lies along either the CCAM line or the CV-ch line, rather than representing a deviation from the porphyritic chondrule trend.

Choi et al. (2000) inferred that the ^{16}O-poor end of the CV chondrite array has values of $\delta^{18}O \sim +10‰$ and $\delta^{17}O \sim +5‰$, with $\Delta^{17}O \sim -1‰$, and our data for chondrule 36 fall very close to this composition. Because barred olivine chondrules are likely to have undergone the most extensive exchange with the nebular gas, it is possible that chondrule 36 represents the most isotopically equilibrated chondrule in CV chondrites that has been analyzed to date.

4.2.4. Al-rich chondrule, 14C

Chondrule 14C is Al-rich, and thus, compositionally, may represent material that is intermediate between CAI and ferromagnesian chondrule material. Our in situ oxygen isotope data address the question of whether Al-rich chondrules contain relict CAI material, and the relationships between these different types of materials. Russell et al. (2000) showed that in unequilibrated ordinary chondrites, individual mineral grains in Al-rich chondrules define a trend that extends from ferromagnesian chondrule compositions towards ^{16}O-rich values. They showed that spinel grains in Al-rich chondrules are not relict grains from CAIs, and concluded that Al-rich chondrules are more closely related to ferromagnesian chondrules than to CAIs. Our data for chondrule 14C agree with these conclusions. In chondrule 14C, we see no evidence that either the olivine or the spinel is relict CAI material because all the grains have values of $\delta^{18}O$ around -5 to -10‰, in the range of most ferromagnesian chondrules. Unlike the data for unequilibrated ordinary chondrites (UOCs), mineral grains in 14C are entirely within the range of mineral grains from ferromagnesian chondrules.

The cores of olivine grains in chondrule 14C are enriched in refractory lithophile elements such as CaO and Al_2O_3, and show bright cathodoluminescence (Fig. 8). Olivine grains with these properties have previously been suggested to be relict condensates (Steele, 1986; Weinbruch et al., 1993, 2000). Our data show that there is no distinguishable difference in oxygen isotopic compositions between the cores and edges of these grains, arguing against the likelihood that the cores are relict condensates, and supporting the arguments that these grains grew from chondrule melts (McSween, 1977b; Jones and Scott, 1989).

Oxygen isotope ratios in olivine in 14C are significantly enriched in ^{16}O compared with the bulk chondrule value (Fig. 7c). We interpret this to indicate that the mesostasis in this chondrule is depleted in ^{16}O relative to olivine. This effect may also be present in chondrule 34, but is probably particularly pronounced in chondrule 14C because of the high proportion of mesostasis. Two possible explanations for the differences between the two phases can be invoked, both of which were discussed above for chondrules 11 and 12. Firstly, it is possible that the mesostasis has been affected by solid-state equilibration with an external reservoir during parent body processing. Bridges et al. (1999) suggested that this mechanism was responsible for a similar effect in chondrules from unequilibrated ordinary chondrites. In Mokoia, the more ^{16}O-poor external reservoir could be the same reservoir that Choi et al. (2000) inferred to be present during formation of magnetite and fayalite in Mokoia, with an oxygen isotope ratio at the high end of the CCAM line and a value of $\Delta^{17}O$ of about -1‰. We discounted this mechanism for producing the oxygen isotope heterogeneity in chondrules 11 and 12, because in those chondrules the heterogeneity is within one mineral phase, olivine. However, in chondrule 14C the heterogeneity appears to be mineral-specific and it is very likely that oxygen isotope exchange would occur more rapidly in feldspar than in olivine and spinel, so we consider this mechanism to be viable. The alternative model for the differences in isotopic compositions between olivine and mesostasis is that oxygen isotope exchange took place between the molten chondrule and the nebula gas, as discussed for chondrules 11 and 12. Because the fractionation is in the same sense as chondrules 11 and 12, and because the distribution in chondrule 14C lies along the same line as the distribution in chondrules 11 and 12, we consider this model to be equally viable.

5. SUMMARY

Bulk chondrule oxygen isotopic compositions for Mokoia span a wider range than any that has been measured for other carbonaceous chondrites, down to $\delta^{18}O$ values around −12‰. The most ^{16}O-rich bulk chondrules are microporphyritic, olivine-rich chondrules in which there is considerable isotopic heterogeneity between individual olivine grains, with extremely ^{16}O-rich olivine grains having $\delta^{18}O$ values around −50‰. This heterogeneity may represent solid-state chemical equilibration of isotopically heterogeneous assemblages that contained relict olivine grains, or it may have been produced by gas-melt isotopic exchange during chondrule formation, during which a changing oxygen isotopic composition became frozen-in to individual olivine grains.

Bulk chondrules in the CV chondrites, Allende and Mokoia, lie on a line with a slope of 0.99 on an oxygen 3-isotope plot that is displaced significantly from the Young and Russell, slope 1.00, "primitive oxygen reservoir" line. The CV-chondrule line defines the most relevant and significant array of oxygen isotopes for chondrules and other components in CV chondrites.

Acknowledgments—We thank S. Itoh and an anonymous reviewer for helpful reviews. We are very grateful to Rae Carey for technical assistance. SEM and electron microprobe work was carried out in the Electron Microbeam Analysis Facility, Department of Earth and Planetary Sciences and Institute of Meteoritics, University of New Mexico. This work was partially supported by NASA grants NAG5-9463 (R.H.J.: J. J. Papike, P.I.) and NAG5-7540 (L.A.L.). T.D. acknowledges support from the Foundation for Polish Science, Warsaw.

Associate editor: S. S. Russell

REFERENCES

Ash R. D, Young E. D (2000). Clarity and confusion: The history of Allende chondrules as evinced by oxygen isotopes. *Lunar Planet. Sci.* **XXXI,** Abstract, 1881 (CD-ROM).

Brearley A. J. (1997) Disordered biopyriboles, amphibole, and talc in the Allende meteorite: Products of nebular or parent body aqueous alteration? *Science* **276,** 1103–1105.

Bridges J. C., Franchi I. A., Sexton A. S., and Pillinger C. T. (1999) Mineralogical controls on the oxygen isotopic compositions of UOCs. *Geochim. Cosmochim. Acta* **63,** 945–951.

Choi B.-G., McKeegan K. D., Leshin L. A., and Wasson J. T. (1997) Origin of magnetite in oxidized CV chondrites: In situ measurement of oxygen isotope compositions of Allende magnetite and olivine. *Earth Planet. Sci. Lett.* **146,** 337–349.

Choi B.-G., Krot A. N., and Wasson J. T. (2000) Oxygen isotopes in magnetite and fayalite in CV chondrites Kaba and Mokoia. *Meteor. Planet. Sci.* **35,** 1239–1248.

Clayton R. N. (1993) Oxygen isotopes in meteorites. *Ann. Rev. Earth Planet. Sci.* **21,** 115–149.

Clayton R. N. (2002) Self-shielding in the solar nebula. *Nature* **415,** 860.

Clayton R. N. and Mayeda T. K. (1984) The oxygen isotope record in Murchison and other carbonaceous chondrites. *Earth Planet. Sci. Lett.* **67,** 151–161.

Clayton R. N., Onuma N., Grossman L., and Mayeda T. K. (1977) Distribution of the pre-solar component in Allende and other carbonaceous chondrites. *Earth Planet. Sci. Lett.* **34,** 209–224.

Clayton R. N., Onuma N., Ikeda Y., Mayeda T. K., Hutcheon I. D., Olsen E. J., and Molini-Velsko C. (1983) Oxygen isotopic compositions of chondrules in Allende and ordinary chondrites. In *Chondrules and Their Origins* (ed. E. A. King), pp. 37–43. Lunar and Planetary Institute, Houston.

Cohen R. E., Kornacki A. S., and Wood J. A. (1983) Mineralogy and petrology of chondrules and inclusions in the Mokoia CV3 chondrite. *Geochim. Cosmochim. Acta* **47,** 1739–1757.

Fagan T. J., McKeegan K. D., Krot A. N., and Keil K. (2001) Calcium-aluminum-rich inclusions in enstatite chondrites (II): Oxygen isotopes. *Meteor. Planet. Sci.* **36,** 223–230.

Freer R. (1990) Mass transport in minerals. *J. Chem. Soc. Faraday Trans.* **86,** 1281–1286.

Guan Y., McKeegan K. D., and MacPherson G. J. (2000) Oxygen isotopes in calcium-aluminum-rich inclusions from enstatite chondrites: New evidence for a single CAI source in the solar nebula. *Earth Planet. Sci. Lett.* **181,** 271–277.

Guimon R. K., Symes S. K., Sears D. W. G., and Benoit P. H. (1995) Chemical and physical studies of type 3 chondrites XII: The metamorphic history of CV chondrites and their components. *Meteoritics* **30,** 704–714.

Hewins R. H, Connolly H. C Jr. (1996). In *Peak temperatures of flash-melted chondrules.* Chondrules and the Protoplanetary Disk (eds. R. H. Hewins, R. H. Jones and E. R. D. Scott), pp. 197-204. Cambridge University Press.

Hiyagon H. and Hashimoto A. (1999) ^{16}O excesses in olivine inclusions in Yamato-86009 and Murchison chondrites and their relation to CAIs. *Science* **283,** 828.

Housley R. M. and Cirlin E. H. (1983) On the alteration of Allende chondrules and the formation of matrix. In *Chondrules and Their Origins* (ed. E. A. King), pp. 145–161. Lunar and Planetary Institute, Houston.

Hua X., Adam J., Palme H., and El Goresy A. (1988) Fayalite-rich rims, veins, and halos around and in forsteritic olivines in CAIs and chondrules in carbonaceous chondrites: Types, compositional profiles and constraints on their formation. *Geochim. Cosmochim. Acta* **52,** 1389–1408.

Hutcheon I. D., Krot A. N., Keil K., Phinney D. L., and Scott E. R. D. (1998) ^{53}Mn-^{53}Cr dating of fayalite formation in the CV3 chondrite Mokoia: Evidence for asteroidal alteration. *Science* **282,** 1865–1867.

Itoh S. and Yurimoto H. (2003) Contemporaneous formation of chondrules and refractory inclusions in the early solar system. *Nature* **423,** 728–731.

Jones R. H, Schilk A. J (2000) Chemistry and petrology of chondrules from the Mokoia CV chondrite. In *Lunar and Planetary Science Conference* **XXXI,** Abstract #1400, Lunar and Planetary Institute, Houston (CD-ROM).

Jones R. H, Scott E. R. D (1989) Petrology and thermal history of type IA chondrules in the Semarkona (LL3.0) chondrite. *Proc. 19th Lunar. Planet. Sci. Conf.* 523-536.

Jones R. H., Saxton J. M., Lyon I. C., and Turner G. (2000) Oxygen isotopic compositions of chondrule olivine and isolated olivine grains in the CO3 chondrite, ALHA77307. *Meteor. Planet. Sci.* **35,** 849–857.

Kimura M. and Ikeda Y. (1996) Comparative study on alteration processes of chondrules in oxidized and reduced CV3 chondrites. *Meteor. Planet. Sci.* **31,** A70–71 (abstr.).

Kimura M. and Ikeda Y. (1998) Hydrous and anhydrous alterations of chondrules in Kaba and Mokoia CV chondrites. *Meteor. Planet. Sci.* **33,** 1139–1146.

Kobayashi S., Imai H. and Yurimoto H. (2003) An extreme ^{16}O-rich chondrule from Acfer 214 CH chondrite. *Lunar Planet. Sci.* **XXXIV,** Abstract #1536 (CD-ROM).

Komatsu M., Krot A. N., Petaev M. I., Ulyanov A. A., Keil K., and Miyamoto M. (2001) Mineralogy and petrography of amoeboid olivine aggregates from the reduced CV3 chondrites Efremovka, Leoville and Vigarano: Products of nebular condensation, accretion and annealing. *Meteor. Planet. Sci.* **36,** 629–641.

Krot A. N., Scott E. R. D., and Zolensky M. E. (1995) Mineralogical and chemical modification of components in CV3 chondrites: Nebular or asteroidal processing? *Meteoritics* **30,** 748–775.

Krot A. N., Scott E. R. D., and Zolensky M. E. (1997) Origin of fayalitic olivine rims and lath-shaped matrix olivine in the CV3 chondrite Allende and its dark inclusions. *Meteoritics* **32,** 31–49.

Krot A. N., McKeegan K. D., Leshin L. A., MacPherson G. J., and Scott E. R. D. (2002) Existence of an ^{16}O-rich gaseous reservoir in the solar nebula. *Science* **295,** 1051–1054.

Lofgren G. E. (1996) A dynamic crystallization model for chondrule melts. In *Chondrules and the Protoplanetary Disk* (eds. R. H. Hewins, R. H. Jones and E. R. D. Scott), pp. 187-196. Cambridge University Press.

Lofgren (2000) Partial melting model for formation of aggregate and porphyritic chondrules. *Meteor. Planet. Sci.* **35,** A99-100 (abstr.).

Lyons J. R, Young E. D (2003) Towards an evaluation of self-shielding at the X-point as the origin of the oxygen isotope anomaly in CAIs. *Lunar Planet. Sci.* **XXXIV,** Abstract # 1981 (CD-ROM), Lunar and Planetary Institute, Houston.

Mayeda T. K., Clayton R. N., and Nagasawa H. (1986) Oxygen isotope variations within Allende refractory inclusions. *Lunar Planet. Sci.* **XVI,** 526–527.

McKeegan KD., Leshin L. A., Russell S. S., and MacPherson G. J. (1998) Oxygen isotopic abundances in calcium-aluminum-rich inclusions from ordinary chondrites: Implications for nebular heterogeneity. *Science* **280,** 414–418.

McSween H. Y., Jr.. (1977a) Petrographic variations among carbonaceous chondrites of the Vigarano type. *Geochim. Cosmochim. Acta* **41,** 1777–1790.

McSween H. Y., Jr.. (1977b) On the nature and origin of isolated olivine grains in carbonaceous chondrites. *Geochim. Cosmochim. Acta* **41,** 411–418.

McSween H. Y., Jr.. (1985) Constraints on chondrule origin from petrology of isotopically characterized chondrules in the Allende meteorite. *Meteoritics* **20,** 523–540.

Morioka M. (1981) Cation diffusion in olivine-II. Ni-Mg, Mn-Mg, Mg and Ca. *Geochim. Cosmochim. Acta* **45,** 1573–1580.

Peck J. A. (1983) Chemistry of CV3 matrix minerals and Allende chondrule olivine. *Meteoritics* **18,** 373–374.

Peck J. A. and Wood J. A. (1987) The origin of ferrous zoning in Allende chondrule olivine. *Geochim. Cosmochim. Acta* **51,** 1503–1510.

Rubin A. E. (1984) Coarse-grained chondrule rims in type 3 chondrites. *Geochim. Cosmochim. Acta* **48,** 1779–1789.

Rubin A. E., Wasson J. T., Clayton R. N., and Mayeda T. K. (1990) Oxygen isotopes in chondrules and coarse-grained chondrule rims from the Allende meteorite. *Earth Planet. Sci. Lett.* **96,** 247–255.

Russell S. S., MacPherson, G. J., Leshin L. A., and McKeegan K. D. (2000) ^{16}O enrichments in aluminum-rich chondrules from ordinary chondrites. *Earth Planet. Sci. Lett.* **184,** 57–74.

Ryerson F. J., Durham W. B., Cherniak D. J., and Lanford W. A. (1989) Oxygen diffusion in olivine: Effect of oxygen fugacity and implications for creep. *J. Geophys. Res.* **94 (***B4***),** 4105–4118.

Schilk A. J (1991) Chemical and statistical analyses of chondrules from the Mokoia (CV3) meteorite. Ph. D. thesis, Oregon State University.

Scott E. R. D., Barber D. J., Alexander C. M. O., Hutchison R., and Peck J. A. (1988) Primitive material surviving in chondrites: Matrix. In *Meteorites and the Early Solar System* (eds. J. F. Kerridge and M. S. Matthews), pp. 718–745. University of Arizona, Tucson, Arizona.

Sharp Z. D. (1990) A laser-based microanalytical method for the in situ determination of oxygen isotope ratios of silicates and oxides. *Geochim. Cosmochim. Acta* **54,** 1353–1357.

Sharp Z. D. (1995) Oxygen isotope geochemistry of the Al_2SiO_5 polymorphs. *Am. J. Sci.* **295,** 1058–1076.

Shu F. H., Shang H., and Lee T. (1996) Towards an astrophysical theory of chondrites. *Science* **271,** 1545–1552.

Steele I. M. (1986) Compositions and textures of relic forsterite in carbonaceous and unequilibrated ordinary chondrites. *Geochim. Cosmochim. Acta* **50,** 1379–1395.

Thiemens M (1996). In *Mass independent isotopic effects in chondrites: The role of chemical processes*. Chondrules and the Protoplanetary Disk (eds. R. H. Hewins, R. H. Jones and E. R. D. Scott), pp. 197-204. Cambridge University Press.

Tissandier L., Libourel G., and Robert F. (2002) Gas-melt interactions and their bearing on chondrule formation. *Meteor. Planet. Sci.* **37,** 1377–1389.

Tomeoka K. and Buseck P. R. (1982) An unusual layered mineral in chondrules and aggregates of the Allende carbonaceous chondrite. *Nature* **299,** 327–329.

Tomeoka K. and Buseck P. R. (1990) Phyllosilicates in the Mokoia CV carbonaceous chondrite: Evidence for aqueous alteration in an oxidizing environment. *Geochim. Cosmochim. Acta* **54,** 1745–1754.

Wasson J. T. (2000) Oxygen-isotopic evolution of the solar nebula. *Rev. Geophys.* **38,** 491–512.

Weinbruch S., Palme H., Müller W. F., and El Goresy A. (1990) FeO-rich rims and veins in Allende forsterite: Evidence for high temperature condensation at oxidizing conditions. *Meteoritics* **25,** 115–125.

Weinbruch S., Zinner E. K., El Goresy A., Steele I. M., and Palme H. (1993) Oxygen isotopic composition of individual olivine grains from the Allende chondrite. *Geochim. Cosmochim. Acta* **57,** 2649–2661.

Weinbruch S., Palme H., and Spettel B. (2000) Refractory forsterite in primitive meteorites: Condensates from the solar nebula? *Meteor. Planet. Sci.* **35,** 161–172.

Wiens R. C., Huss G. R. and Burnett D. S. (1999) The solar oxygen-isotopic composition: Predictions and implications for solar nebula processes. *Meteoritics Planet. Sci.* **34,** 99-107.

Young E. D. and Russell S. S. (1998) Oxygen reservoirs in the early solar nebula inferred from an Allende CAI. *Science* **282,** 452–455.

Young E. D., Coutts D. W., and Kapitan D. (1998) UV laser ablation and irm-GCMS microanalysis of ^{18}O/^{16}O and ^{17}O/^{16}O with application to a calcium-aluminum-rich inclusion from the Allende meteorite. *Geochim. Cosmochim. Acta* **62,** 3161–3168.

Young E. D., Ash R. D., Galy A., and Belshaw N. (2002) Mg isotope heterogeneity in the Allende meteorite measured by UV laser ablation-MC-ICPMS and comparisons with O isotopes. *Geochim. Cosmochim. Acta* **66,** 683–698.

Yu Y., Hewins R. H., Clayton R. N., and Mayeda T. K. (1995) Experimental study of high temperature oxygen isotope exchange during chondrule formation. *Geochim. Cosmochim. Acta* **59,** 2095–2104.

Yurimoto H. and Kuramoto K. (2002) A possible scenario introducing heterogeneous oxygen isotopic distribution in proto-planetary disks. *Meteor. Planet. Sci.* **37,** A153 (abstr.).

Yurimoto H. and Wasson J. T. (2002) Extremely rapid cooling of a carbonaceous-chondrite chondrule containing very ^{16}O-rich olivine and a ^{26}Mg excess. *Geochim. Cosmochim. Acta* **66,** 4355–4363.